Low Velocity Quantum Reflection of Bose-Einstein Condensates

T. A. Pasquini, M. Saba, G.-B. Jo, Y. Shin, W. Ketterle, and D. E. Pritchard
*Department of Physics, MIT-Harvard Center for Ultracold Atoms, and Research Laboratory of Electronics, Massachusetts Institute of Technology, Cambridge, Massachusetts 02139, USA**

T. A. Savas
NanoStructures Laboratory and Research Laboratory of Electronics, Massachusetts Institute of Technology, Cambridge, Massachusetts 02139, USA

N. Mulders
Department of Physics, University of Delaware, Newark, Delaware 19716, USA
(Received 15 March 2006; published 30 August 2006)

We study how interactions affect the quantum reflection of Bose-Einstein condensates. A patterned silicon surface with a square array of pillars resulted in high reflection probabilities. For incident velocities greater than 2.5 mm/s, our observations agreed with single-particle theory. At velocities below 2.5 mm/s, the measured reflection probability saturated near 60% rather than increasing towards unity as predicted by the accepted theoretical model. We extend the theory of quantum reflection to account for the mean-field interactions of a condensate which suppresses quantum reflection at low velocity. The reflected condensates show collective excitations as recently predicted.

DOI: 10.1103/PhysRevLett.97.093201 PACS numbers: 34.50.Dy, 03.75.Kk

Recent years have seen an explosive growth of experiments with cold atoms near surfaces, driven by the desire to miniaturize atomic physics experiments using so-called ''atom chips'' [1], for practical applications in magnetometry [2] and atom interferometry [3]. The Casimir-Polder interaction becomes important close to the surface an atom chip [4–6] and offers both fundamental and technical relevance. Fundamental studies include the use of Bose-Einstein condensates to determine the Casimir-Polder potential [7,8], to observe its modification by thermal radiation [9], and the intriguing question if unity quantum reflection can be achieved at extremely low temperatures. Quantum reflection is the phenomena by which an atom is accelerated so violently by the attractive surface potential that it reflects from the potential rather than being drawn into the surface [10–13]. Current models of quantum reflection treat the atom-surface interaction as a single-atom potential, and predict a monotonic rise to unity reflection at zero velocity. However, in a recent study of quantum reflection of Bose-Einstein condensates (BECs) [14], the reflection probability saturated at ~12% at low velocity [15]. A Letter simulating quantum reflection of BECs demonstrated excitations during reflection as a result of mean-field interactions but could not explain the low reflectivity [16].

In this work, we address how quantum reflection of BECs differs from the reflection of single atoms and discuss the role of interatomic interactions before, during, and after reflection. Compared to our previous study, where some effects of interactions were already observed but not characterized or explained [14], we are now more sensitive, having improved the reflection probability to 67% by using a pillared silicon surface, in the spirit of experiments with grazing-incidence neon atoms on ridged silicon [17–19]. In contrast to single-particle theory, we observe a saturation of the reflection probability at low incident velocity, suggesting that the description of quantum reflection is incomplete. We propose a simple theoretical extension incorporating a mean-field potential which is found to dramatically suppress the reflection probability near zero velocity. Further, we observe that interactions between the incident and reflected condensate lead to predicted collective excitations of the reflected condensate [16] and incoherent scattering.

Bose-Einstein condensates of ^{23}Na atoms were prepared and transferred into a loosely confining gravitomagnetic trap, comprising a single coil and three external bias fields, as described in Ref. [20]. For typical loading parameters, condensates with $N \approx 1 \times 10^6$ atoms were confined ~1 cm above the coil in a harmonic trap characterized by angular frequencies $(\omega_\perp, \omega_y, \omega_z) = 2\pi \times (4.2, 5.0, 8.2)$ Hz, where directions $(\perp, y, z)$ are defined in Fig. 1. At this point, $\omega_\perp$ and ω_y were adjusted by changing the vertical bias field as described in Ref. [20]. Typical densities in the trap were $\sim 5 \times 10^{12}$ cm^{-3} and diameters were ~150 μm. A silicon surface attached to a micrometric, motorized linear actuator was mounted ~1 cm above the single coil. The position of the surface relative to the center of the coil was adjustable during the experiment as shown in Fig. 1(a).

The surface used in this experiment, provided by the MIT Nanostructures Laboratory, was a pillar structure etched into single-crystal silicon. The structure was created by interference lithography and various subsequent etching

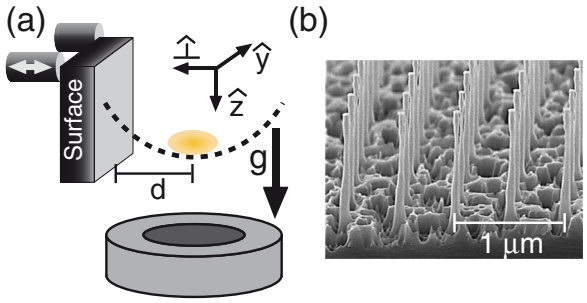

FIG. 1 (color online). Experimental schematic. (a) Atoms were confined in a gravitomagnetic trap near a pillared Si surface. Atoms were accelerated towards the surface by displacing the trapping potential a distance d (greatly exaggerated) so that it was centered on the surface. The surface was mounted on a translation stage and could be removed at any point for imaging. (b) Scanning electron micrograph of the pillared Si surface used in this experiment.

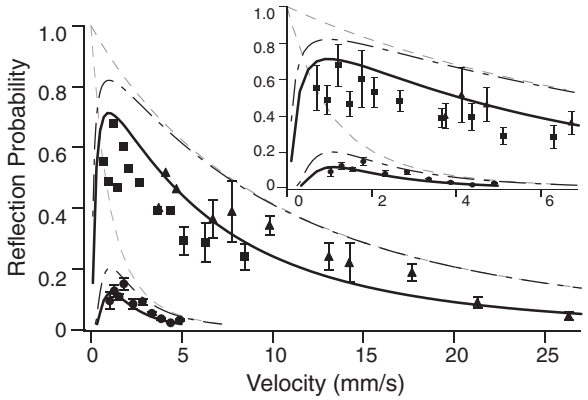

FIG. 2. Reflection probability vs incident velocity. Data were collected in a magnetic trap with trap frequencies $2\pi \times (2.0, 2.5, 8.2)$ Hz (squares) and $2\pi \times (4.2, 5.0, 8.2)$ Hz (triangles). For comparison, data from Ref. [14] for reflection off a solid silicon surface are shown as circles. Incident and reflected atom numbers were averaged over several shots. For clarity error bars for data below 5 mm/s are shown only in the inset plot, which has a different horizontal axis to emphasize the low velocity data. Systematic uncertainty in the velocity due to residual motion is approximately 10%. Theoretical curves are described in the text.

steps [21–23]. Figure 1(b) shows the final surface as an array of 1 μm tall, 50 nm diameter pillars spaced at 500 nm. Such a surface should provide a Casimir potential approximately 1% of the value for a solid Si surface. A dilute surface is expected to exhibit enhanced quantum reflection.

Studying the reflection properties of the surface requires a controlled collision. After loading the condensate into the trap, the surface was moved to a desired distance d from the trap center. By changing the bias field $B_\perp$ appropriately, a dipole oscillation centered on the surface was induced [14]. After waiting $T_\perp/4 = 2\pi/4\omega_\perp$ the atoms hit the surface with velocity $v_\perp = d\omega_\perp$. By varying $\omega_\perp$ between $2\pi \times 2$ and $2\pi \times 4$ Hz and d over 50 μm to 1 mm, velocities in the range of 0.5 to 26 mm/s could be studied. The reflection probability was calculated as the ratio of the average reflected atom number to the average incident atom number [24]. The reflection probability along with data for a solid silicon surface [14] are shown in Fig. 2. The pillared surface shows higher reflectivity over a wider range of incident velocity, as expected. The reflection maximum is 67% for a velocity of 1.2 mm/s, and reflection probabilities above 10% were measured at velocities up to 20 mm/s. Below ~3 mm/s, the reflection probability flattens near 55%, qualitatively similar to the behavior of the solid surface where the reflectivity flattened near 12% in the same velocity range.

Reflection probabilities for a single atom were calculated by numerically solving the Schrödinger equation for a 1D potential [25]. The surface potentials of the Casimir-Polder form C_4/r^4 are obtained using $C_4^{\mathrm{Si}} = 6.2 \times 10^{-56}$ J m^4 for bulk silicon [26] and combining contributions from both the pillar layer and the bulk substrate. We average the density of the material before calculating the potential, simulating the surface as a 1 μm thick overlayer of material with $C_4 = 0.01 \times C_4^{\mathrm{Si}}$ added to a semi-infinite slab of material with $C_4 = C_4^{\mathrm{Si}}$. The resulting reflection probability curve is shown in Fig. 2 as dashed gray lines. A model which averages the 3D potential of the pillars to obtain a 1D potential shows similar results. Further, these simulations show that the reflection probability depends mainly on the diluted pillar layer and only weakly on the bulk material underneath or the height or arrangement of the pillars. Unlike grazing-incidence experiments [17–19], here the de Broglie wavelength, $\lambda_{\mathrm{dB}} \simeq 1$ μm, exceeds the spacing of the pillars and we are insensitive to the surface structure.

Calculations predict that the reflection probability approaches unity for low incident velocity. This is in contrast to our observation that the reflection probability saturates below 2.5 mm/s for both the pillared and solid surfaces. It was suggested that this saturation is due to low velocity excitations which smear out the condensate density; although the reflectivity approaches unity, some reflected atoms would appear in a diffuse cloud which may fall below a detection threshold [16]. However, this could explain our previous results [14] only when we assume a density threshold for detection of $0.25 \times n_0 \approx 10^{12}$ cm^{-3}, where n_0 is the central condensate density, which is 20 times higher than the lowest densities we are able to detect [20].

There is a finite-size correction to the standard description of quantum reflection, but it is too small to account for our observations. For an incident atom cloud of size d, the smallest incident velocity is h/md, approximately 0.2 mm/s for our parameters. We conclude that a single-particle description cannot account for our low velocity data and now discuss possible effects due to the condensate's mean-field interaction.

The mean-field potential is taken to be that of a condensate at rest with a fully reflecting wall as a boundary

condition. The condensate's density decays towards zero at the wall over a characteristic length scale given by the healing length, ξ. The atoms at the edge of the condensate thereby acquire a velocity given by $\approx h/m\xi$, which is approximately equal to the speed of sound c. If the healing length is much larger than the relevant range of the Casimir-Polder potential, approximately 1 μm as defined by the so-called badlands region [13], one would assume that the mean-field potential simply accelerates the atoms. Atoms leaving the condensate enter the region of quantum reflection with an incident velocity obtained from $mv^2/2 = U = mc^2$. This model would shift the single-atom quantum reflection curves by the velocity $v = \sqrt{2}c$, which is ≈ 1.5 mm/s for our parameters. This shift is too small to explain the low reflectivity at our lowest velocities. Additionally, the assumption that the healing length be much larger than the distance at which quantum reflection occurs is not valid for our data.

In order to fully account for interaction effects, we calculate the quantum reflection probability using a composite potential which includes both the Casimir-Polder potential and the mean-field potential [Fig. 3(a)]. The predicted reflection probability is shown in Fig. 3(b). At high velocities (>3 mm/s), quantum reflection occurs close to the surface where the mean-field potential plays no role. As the velocity is reduced, the point of reflection moves outward, into the region where the mean-field potential "softens" the Casimir-Polder potential, dramatically reducing the reflectivity. At very low velocities (<0.1 mm/s), when the badlands region is far from the surface, the predicted reflection resembles the reflection probability from the mean-field potential of the condensate rather than from the Casimir-Polder potential and becomes unity at zero velocity [15]. This model predicts well, without any free parameter, the velocities below which we have observed saturation of the reflectivity for both the solid and pillared surface as shown by the dot-dashed lines in Fig. 2. The data do not extend far enough into the very low velocity regime to confirm the model's prediction of a sharp drop.

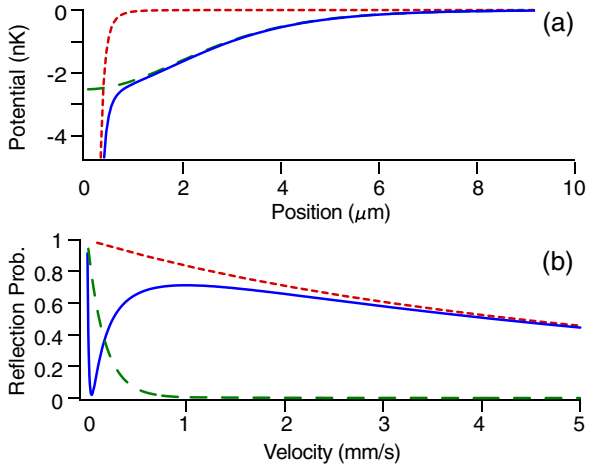

FIG. 3 (color online). Mean-field model for quantum reflection of condensates. (a) The trapped condensate provides a repulsive mean-field energy which is a constant away from the surface and, within the healing length ξ, drops to zero. The dashed curve shows this mean-field potential set to zero at infinity. This potential combined with the Casimir potential (dotted curve) creates the composite potential (solid curve) which we use to model reflection in the presence of a condensate. (b) The reflection probabilities from the same potentials for low velocities.

The model does not include the effects of the moving condensate, its observed collective excitations, or the distortion of the condensate wave function by surface attraction or the loss of atoms to the surface.

The calculated curves are not in quantitative agreement with the experimental data; the observed reflection probabilities are lower, even at high velocity. A possible explanation is the modification of the potential by stray electric fields, caused by sodium atoms deposited on the surface (adatoms). Recently, the partial ionization of rubidium adatoms by bulk silicon has been shown empirically to produce an electric field of several V/cm at 10 μm from the surface [5]. This electric field, which falls off as $1/r^2$, will produce an additional potential, $V_A(r) = -A/r^4$, which will reduce the reflection probability. To account for stray electric fields, we fit the high velocity data for the pillared (solid) surface using a potential $V_{\mathrm{tot}} = -0.01 \times C_4^{\mathrm{Si}}/r^4 - A/r^4$ ($V_{\mathrm{tot}} = -C_4^{\mathrm{Si}}/r^4 - A/r^4$). We find for the pillared (solid) surface a value of A of $0.02 \times C_4^{\mathrm{Si}}$ (C_4^{Si}) corresponding to a stray field $\sim$10 V/cm ($\sim$70 V/cm) at 1 μm, which scales to 0.1 V/cm (0.7 V/cm) at 10 μm, smaller than measured for rubidium. We may expect a greater factor between the fields measured for a solid and dilute surface owing to the factor of 100 difference in surface area. However, the strength of the fields depends on the specific geometry, surface material, and contamination level, which may vary between the two experiments. Because of experimental limitations, we were not able to confirm the magnitude of these stray fields or their sole responsibility for the observed discrepancy, and include their effect as a phenomenological fitting parameter for the high velocity data.

If we combine the stronger surface potential with the mean-field potential, we have a phenomenological model which is consistent with all our data, shown in Fig. 2 as solid lines. It would be very interesting to test this model by varying the density over a large range and try to observe the predicted decrease of the saturation velocity for lower density. We could not study reflection at lower density due to a rapid decrease of the signal-to-noise ratio.

Another aspect of interactions are collisions between incident and reflected parts of the condensate. This leads to a standing wave during the collision, for a time inversely proportional to the incident velocity. As this time becomes comparable to the transverse and vertical trap periods, vortex rings, solitons, and other excitations may form, distorting the cloud [16]. In our experiment, this veloc-

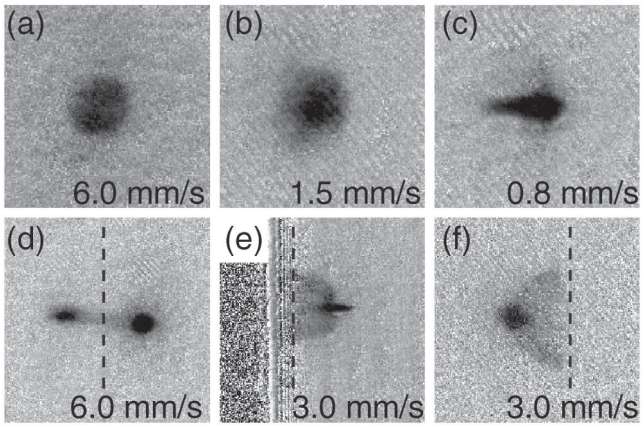

FIG. 4. Menagerie of reflection effects. (a)–(c) As the incident velocity is reduced, the reflected condensate becomes increasingly excited. (d) By removing the surface at the moment of reflection, we can see both the incident (left) and reflected (right) condensates. The reflection probability is 30%. (e) The collision of the incident and reflected condensates produces a strong s-wave scattering halo at low velocity, visible here $T_\perp/4$ after reflection. The surface is still present on the left in this image. Half of the halo is missing due to surface reflection or absorption. (f) With the surface removed, the scattered atoms remain in the trap after an additional half trap period and appear reversed in position and velocity. Field of view for images (a)–(c) is 540 μm and for (d)–(f) is 800 μm; the dashed line is the position of the surface (moved for imaging) at the moment of reflection.

ity is approximately 2 mm/s. The higher reflection efficiency of the pillared surface in excess of 50% allowed us to observe these collective effects. At high velocities (>4 mm/s), we observe that the reflected cloud appears, apart from diminished size and number, similar to the bimodal distribution of the incident cloud, shown in Fig. 4(a). As the incident velocity is reduced, as in Figs. 4(b) and 4(c), the cloud develops a complex surface mode excitation [27].

Further, we observe elastic s-wave scattering between atoms in the incident and reflected condensates leading to halos [28,29], which we observe after a hold time $T_\perp/4$ [Figs. 4(e) and 4(f)].

We also performed the experiment using an aerogel surface. Aerogels are electrically insulating, randomly structured, silica foams with a density of $\sim$2% of bulk silica [30] and should display reflection properties similar to the pillared surface. We were unable to observe quantum reflection above our detection threshold of $\sim$2%, an effect we attribute to uncontrolled patch charges which strongly distort the Casimir-Polder potential.

We conclude with an outlook on how to further increase the reflection probability for condensates. Our model predicts improvements for longer healing lengths. Improvements to the reflectivity could also be made by further reducing the density of the surface and would require further advances in fabrication techniques.

This work was supported by NSF, ONR, DARPA, and NASA. We thank S. Will for experimental assistance, M. Zwierlein for experimental suggestions, and R. Scott and M. Fromhold for useful discussions.

*Electronic address: http://cua.mit.edu/ketterle_group/

[1] R. Folman *et al.*, Adv. At. Mol. Opt. Phys. **48**, 263 (2002).
[2] S. Wildermuth *et al.*, Nature (London) **435**, 440 (2005).
[3] Y. Shin *et al.*, Phys. Rev. A **72**, 021604(R) (2005).
[4] D. M. Harber *et al.*, J. Low Temp. Phys. **133**, 229 (2003).
[5] J. M. McGuirk *et al.*, Phys. Rev. A **69**, 062905 (2004).
[6] Y. J. Lin *et al.*, Phys. Rev. Lett. **92**, 050404 (2004).
[7] D. M. Harber *et al.*, Phys. Rev. A **72**, 033610 (2005).
[8] H. Oberst *et al.*, Phys. Rev. A **71**, 052901 (2005).
[9] M. Antezza, L. P. Pitaevskii, and S. Stringari, Phys. Rev. Lett. **95**, 113202 (2005).
[10] D. P. Clougherty and W. Kohn, Phys. Rev. B **46**, 4921 (1992).
[11] C. Carraro and M. W. Cole, Prog. Surf. Sci. **57**, 61 (1998).
[12] A. Mody *et al.*, Phys. Rev. B **64**, 085418 (2001).
[13] H. Friedrich, G. Jacoby, and C. G. Meister, Phys. Rev. A **65**, 032902 (2002).
[14] T. A. Pasquini *et al.*, Phys. Rev. Lett. **93**, 223201 (2004).
[15] The reflection probability $\sim$50%, inferred by measuring the lifetime of atoms confined against a silicon surface [14], may be a result of reflection from the mean-field potential at the edge of the condensate rather than from the Casimir-Polder potential of the surface.
[16] R. G. Scott *et al.*, Phys. Rev. Lett. **95**, 073201 (2005).
[17] F. Shimizu and J. Fujita, J. Phys. Soc. Jpn. **71**, 5 (2002).
[18] H. Oberst *et al.*, Phys. Rev. Lett. **94**, 013203 (2005).
[19] D. Kouznetsov and H. Oberst, Phys. Rev. A **72**, 013617 (2005).
[20] A. E. Leanhardt *et al.*, Science **301**, 1513 (2003).
[21] H. I. Smith *et al.*, J. Vac. Sci. Technol. B **9**, 2992 (1991).
[22] M. L. Schattenburg, R. J. Aucoin, and R. C. Fleming, J. Vac. Sci. Technol. B **13**, 3007 (1995).
[23] T. A. Savas *et al.*, J. Vac. Sci. Technol. B **14**, 4167 (1996).
[24] Atom numbers were obtained by optically pumping the atoms from the state $|F = 1\rangle$ to $|F = 2\rangle$. After a wait time of $\sim$2 ms to allow optically dense regions of the cloud to expand, the distributions were imaged using the $|F = 2\rangle$ to $|F = 3\rangle$ cycling transition.
[25] F. Shimizu, Phys. Rev. Lett. **86**, 987 (2001).
[26] Z. C. Yan, A. Dalgarno, and J. F. Babb, Phys. Rev. A **55**, 2882 (1997).
[27] A movie of reflection is available at http://cua.mit.edu/ketterle_group/Animation_folder/QRMovie.wmv.
[28] K. Gibble, S. Chang, and R. Legere, Phys. Rev. Lett. **75**, 2666 (1995).
[29] A. P. Chikkatur *et al.*, Phys. Rev. Lett. **85**, 483 (2000).
[30] J. Fricke and A. Emmerling, J. Am. Ceram. Soc. **75**, 2027 (1992).